Microporous and Mesoporous Materials 294 (2020) 109855

Contents lists available at ScienceDirect

Microporous and Mesoporous Materials

journal homepage: http://www.elsevier.com/locate/micromeso

Esterification of linoleic acid using HZSM-5 zeolites with different Si/Al ratios

Elyssa G. Fawaz [a], Darine A. Salam [a,*], T. Jean Daou [b,c]

[a] Department of Civil and Environmental Engineering, Maroun Semaan Faculty of Engineering and Architecture, American University of Beirut, P.O.Box: 11-0236, Riad El Solh, Beirut, Lebanon
[b] Université de Haute Alsace, Axe Matériaux à Porosité Contrôlée (MPC), Institut de Science des Matériaux de Mulhouse (IS2M), UMR CNRS 7361, ENSCMu, 68093, Mulhouse, France
[c] Université de Strasbourg, Strasbourg, France

ARTICLE INFO

Keywords:
Zeolites
Si/Al
Transesterification
Acidity
Hydrophobicity

ABSTRACT

Microporous HZSM-5 zeolite crystals of distinct Si/Al ratios (53, 33.3 and 14.4) were compared for linoleic acid esterification with methanol as a model reaction for the production of biodiesel. As-synthesized catalytic materials were characterized using XRD, SEM, TEM, N_2 sorption, X-Ray fluorescence, FTIR, and ^{27}Al MAS NMR. The results showed that HZSM-5 with higher acidity and lower Si/Al ratio achieved high linoleic acid conversions at earlier stages of the reaction, whereas more hydrophobic zeolites reached higher conversions as reaction time increased. A maximum methyl linoleate yield of 79.78% was achieved for the esterification of linoleic acid using HZSM-5 (Si/Al = 53) at 4 h reaction time, 6:1 methanol to linoleic acid molar ratio, 10 wt% catalyst loading and 180 °C. Linoleic acid is activated by being adsorbed on the acid sites of the zeolite surface with increased Si/Al ratios and reacts to form the corresponding methyl ester.

1. Introduction

On account of the high demand for diesel fuel and the adverse effects of its direct combustion on health and the environment, the production of biodiesel and its application have been increasing worldwide as a substitute for conventional petroleum diesel [1,2]. Biodiesel production is traditionally accomplished by fatty acids (FAs) esterification and by triglycerides transesterification from various oil feedstocks, with a short-chain alcohol in excess as methanol, in the presence of a homogeneous base or acid catalyst [3]. However, large amounts of wastewater are generated during biodiesel purification using homogeneous catalysts, increasing thus the costs [4]. Other problems associated with homogeneous catalysts include difficult catalysts separation from the reaction mixture [5,6]. Heterogeneous insoluble acid catalysts minimize the problems associated with homogeneous catalysis. They are easily filtered and used numerous times after recycling [7]. They are also non-corrosive, don't promote soap formation and remove the step of product purification offering thus, a more environmental and economic pathway for biodiesel production [8]. Park et al. [9] compared acid solid tungsten oxide zirconia, amberlyst 15, and sulfated zirconia catalysts for biodiesel production from waste frying oils (WFOs) and recorded highest yield for tungsten oxide zirconia (WO_3/ZrO_2). Feng et al. used the cation exchange resins D61, 001x7 and NKC-9 as acid heterogeneous catalysts in biodiesel production from WFOs. NKC-9 had the best catalytic activity yielding 90% conversion [10]. Gardy et al. produced mesoporous $TiO_2/PrSO_3H$ solid acid catalyst (4.5 wt%) for the transesterification of WFOs which yielded 98.3% biodiesel at 60 °C [11].

ZSM-5 zeolite, which is most commonly synthesized using the hydrothermal route [12], is constituted of channels defined by 10-membered rings and of medium pore (5.1–5.6 Å) [13]. In reason of its exclusive structural network, ion exchangeability, thermal stability, solid acidity, and shape selectivity, ZSM-5 has been extensively consumed in the petrochemical industry as catalyst [14]. The catalytic characteristics of zeolites are usually affected by their physical and chemical properties. Some studies reported that the conversion of oil molecules decreases with increasing the acid zeolite Si/Al ratio [7,15,16]. The concentration of acid sites decreases as the Si increases over Al in the framework of the zeolite reducing thus its catalytic activity. Chung et al. [7] evaluated the acidic properties and the performance of HZSM-5 with various Si/Al ratios on the esterification of free fatty acids (FFAs). The conversion of FFAs decreased with increasing Si/Al molar ratio. The same pattern was reported by Meng et al. [16] whereby

* Corresponding author.
E-mail address: ds40@aub.edu.lb (D.A. Salam).

https://doi.org/10.1016/j.micromeso.2019.109855
Received 19 February 2019; Received in revised form 28 October 2019; Accepted 29 October 2019
Available online 1 November 2019

HZSM-5 with low Si/Al ratios were appropriate for propylene and butylene formation. However, other studies found that zeolites have better catalytic performance in transesterification reactions, with high Si/Al ratios [17–19] as the strength of the acid sites increases despite their lower number in comparison with zeolites of low Si/Al ratios. Doyle et al. [18] assessed the esterification of oleic acid over zeolite catalysts of various Si/Al ratios. The activity of oleic acid over the catalyst with the higher Si/Al ratio improved as the acid strength and catalyst hydrophobicity increases. Tarach et al. [19] also attributed the enhanced activity of highly siliceous HZSM-5 zeolite to its high acid strength. In the present study, acidic properties and Si/Al ratio of HZSM-5 zeolite catalysts effect on the esterification of linoleic acid for biodiesel production as a model reaction was discussed. The catalytic behavior of HZSM-5 zeolites of Si/Al ratios of 14.4, 33.3, and 53 was assessed by varying catalyst loading, methanol to linoleic acid molar ratio, reaction temperature and reaction time. The external mass transfer limitation of HZSM-5 zeolites was investigated and the correlation between the surface hydrophobicity and acidity of the different Si/Al ratios-zeolites with their catalytic activity was evaluated based on experimental results.

2. Experimental section

2.1. Catalysts synthesis

ZSM-5 zeolite (Si/Al = 53) was synthesized by dissolving 0.26 g of sulfuric acid (Aldrich) and 3.19 g of tetraethoxysilane (TEOS, Aldrich, 98%) in 10.75 g of distilled water in a 45 ml stainless-steel ®teflon-lined autoclave. 0.36 g of sodium hydroxide (Riedel de Haen, 99%) and 0.1 g of $Al_2(SO_4)_3.18H_2O$ (Rectapur, 99%) were supplemented to the mixture. An amount of 3.03 g of tetrapropylammonium hydroxide (TPAOH) aqueous solution (25 wt%, Fluka) was finally added to obtain a gel molar composition of: $100SiO_2$: $1Al_2O_3$: $30Na_2O$: $18H_2SO_4$: 20TPAOH: $4000H_2O$ [20]. The gel was then stirred at 1000 rpm during 30 min, heated at 60 °C for 4 h and finally placed in a 30-rpm tumbling oven for 4 days at 150 °C.

ZSM-5 zeolite (Si/Al = 33.3) were synthesized following a modified method developed by Kim and Kim [19].To achieve a molar composition of $100SiO_2$: $2Al_2O_3$: $10Na_2O$: $2250H_2O$, 9.39 g of colloidal silica (Sigma-Aldrich, LUDOX HS 40 wt% SiO_2 in water) and 3.27g of NaOH (10 wt% in water) were added to 5.12 g of distilled water in an autoclave. The mixture was stirred at 200 rpm for 3 h, at room temperature. In a separate beaker, 0.28 g of NaOH (10 wt% in water) and 0.24 g of sodium aluminate ($NaAlO_2$ of 53 wt% Al_2O_3, 42 wt% Na_2O, and 5 wt% H_2O) were dissolved in 9.87 g of distilled water and stirred at 200 rpm for 3 h. An amount of 4.67 g of distilled water were then added to the beaker mixture. At the end of the 3 h, the beaker content was added to the solution present in the teflon-lined stainless-steel autoclaves, and the gel was set aside for 1 h at room temperature, under stirring. The reaction temperature was then increased to 190 °C for 2 h under stirring and finally put in an oven for 35 h at 150 °C.

For comparison, commercial ZSM-5 zeolite (Si/Al = 14.4) was purchased.

To change the produced ZSM-5 zeolites from their Na^+ form to NH_4^+ form, 1 g of prepared Na-ZSM-5 zeolites was added to 20 ml of 1 M solution of NH_4Cl at 80 °C for 2 h under stirring and by reflux. The ion exchange process was repeated three times. NH_4^+-type zeolites were separated by filtration, washed and dried at 105 °C for 6 h the samples were finally calcined in air at 550 °C for 10 h to give zeolites in H^+ form. The synthesized zeolites (H-ZSM5) were represented by their respective Si/Al ratios in the parenthesis following each zeolite name: HZSM-5 (53), HZSM-5 (33.3) and HZSM-5 (14.4).

2.2. Catalysts characterization

A PANalytical MPD X'Pert Pro diffractometer equipped with an X'Celerator real-time multi-strip detector (2.122° 2θ active length) and operating with Cu Kα radiation (λ = 0.15418 nm) was used to obtain the patterns of the X-ray diffraction (XRD) and purity of the produced zeolites. The zeolite diffractogram was recorded at 22 °C in the low range $0.5 < 2\theta < 5°$ and wide range $3 < 2\theta < 50°$ (220 s time step and 0.017° 2θ angle step).

Homogeneity and morphology of the produced crystals were examined by 7 kV accelerating voltage scanning electron microscopy (SEM) (Philips XL 30 FEG microscope).

Nitrogen adsorption-desorption isotherms were carried out with a Micromeritics ASAP 2420 MP instrument at −196 °C. Prior to each experiment, around 50 mg of calcined samples were outgassed to a residual pressure of less than 0.8 Pa at 300 °C for 15 h. Equivalent specific surface areas were calculated using BET equation ($10^{-6} < p/p° \leq 0.05$) according to the criteria given by Walton and Snurr [22] and micropore volumes were obtained from the *t*-plot method [21].

X-ray fluorescence (XRF, Philips, Magic X) was used to determine the samples Si/Al molar ratio and to evaluate their successful exchange.

Pyridine adsorption trailed by infrared spectrometry in a Thermo Nicolet Magna 550-FT-IR spectrometer were used to measure the quantities of Lewis and Brønsted acid sites. Samples of zeolite were squeezed into self-supported pellets of 20 mg. Each wafer was then preheated at 450 °C in an analysis cell for 12 h, in air. The cell was later placed under vacuum for 1 h to eliminate physisorbed molecules, subsequent to decreasing the temperature to 200 °C under air. Prior to introducing pyridine in the cell for 5 min, the temperature was decreased to 150 °C. The amounts of Brønsted [$PyrH^+$] and Lewis [PyrL] acid sites were established using extinction coefficients previously determined by Guisnet et al. [24], following integrating peaks areas at 1545 cm^{-1} and 1454 cm^{-1} respectively.

^{27}Al (I = 5/2) magic angle spinning (MAS) NMR was carried out with a Bruker Avance II 400 spectrometer operating at $B_0 = 9.4$ T (Larmor frequency $\nu_0 = 104.2$ MHz) equipped with a Bruker 2.5 mm double channel probe. The rotor was spun at 25 kHz, and free induction decays (FID) were collected with a p/12 rf pulse (0.6 ms) and a recycle delay of 1 s. Measurements were carried out with $[Al(H_2O)_6]^{3+}$ as an external standard reference [23]. The decompositions of the spectra were performed using the DMFit software [26] in order to determine the Si/Al ratio of the framework (coupled with XRF results).

2.3. Esterification reaction procedure

Linoleic acid (ACROS, 99%) conversion into methyl linoleate in methanol presence was adopted as a biodiesel production model reaction. Experiments were carried out by triplicates in thermostatic oil bath by reflux and under stirring at 550 rpm in 50 ml reactors. Increased quantities of methanol (Riedel De Haen, 99.9%) were added to 0.6 mL of linoleic acid (equivalent to 1 mol, 0.54 g), in order to achieve methanol to linoleic acid molar ratios of 6:1, 12:1 and 25:1. Optimization of reaction temperature was done by performing reactions at 60, 140 and 180 °C, respectively. The effect of different Si/Al ratios of the chemically modified zeolites on fatty acid methyl esters (FAMEs) production was investigated by using catalysts in loadings of 10 wt% relatively to the quantity of linoleic acid. The needed loading of catalyst was dried before the reaction at 105 °C. The esterification reaction kinetics were also studied under the same conditions using the optimal determined methanol to oil molar ratio and reaction temperature.

At the end of the reactions, the reactors were extracted by two dichloromethane (DCM) (Fisher, 99.8%) aliquots of 50 mL each, following their extraction with 50 ml methanol. The liquid extracts were separated from the solid catalysts by gravity filtration through a bed of filtration beads and 0.2 μm filter paper and analyzed for methyl esters and residual linoleic acid.

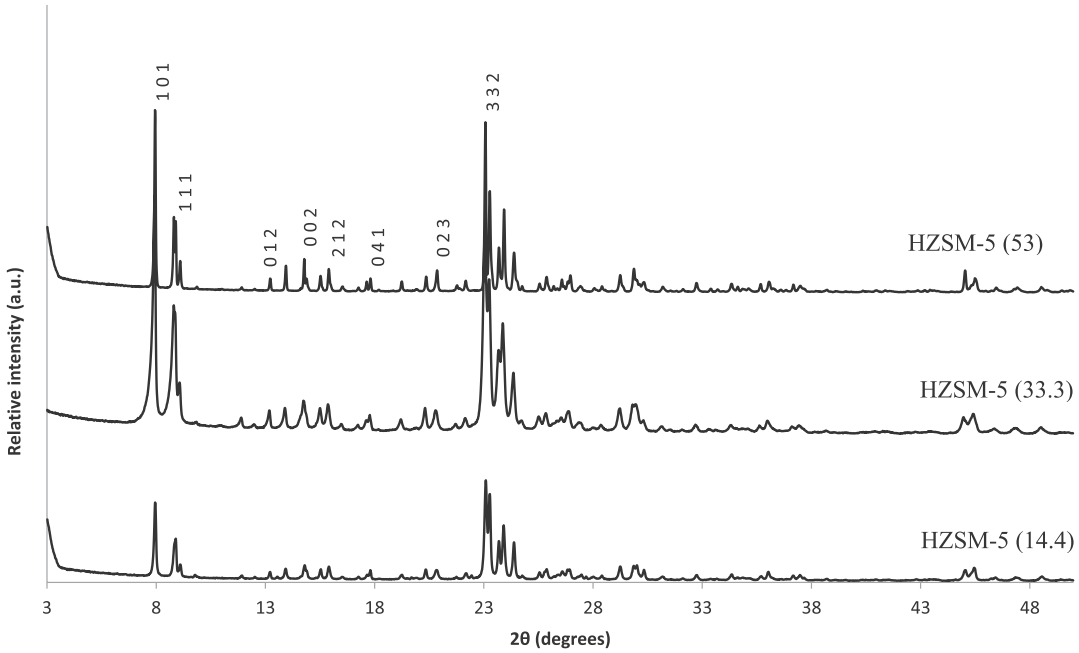

Fig. 1. Wide angle XRD patterns of exchanged and calcined HZSM-5 (53), HZSM-5 (33.3), and HZSM-5 (14.4).

2.4. Method of analysis

Gas chromatography (GC) analysis (Trace Ultragas chromatogram) was used to obtain methyl linoelate content in the liquid extracts. The GC was equipped with a HP-INNOWAX capillary column (30 m × 250 μm × 0.25 μm) and a flame ionization detector (FID). The FID was set at 300 °C, the injector temperature was 250 °C at splitless conditions, and the injection volume of the sample was 5 μl. Helium was used as carrier gas at 1 mL/min. After the isothermal period (2 min at 60 °C), the oven temperature was increased from 60 °C to 200 °C at a 10 °C/min heating rate, and lastly increased to 240 °C at a 5 °C/min ramp and remained for 7 min. Peaks of methyl esters (namely Methyl linoleate among other methyl esters) were identified based on reference standards (Supelco 37 component FAMEs mix in DCM, TraceCert). Equation (1) was employed to find the esterification reaction yield:

$$Yield\ (\%) = \frac{\sum C_{ME} \times V_{extract}}{M_{0\ Linoleic\ acid}} \times 100 \quad (1)$$

where, C_{ME} is the concentration of methyl esters in g/L quantified by GC/FID, $V_{extract}$ is the extract volume (L), and $M_{0\ Linoleic\ acid}$, the initial mass of linoleic acid added to the reactor (0.54 g).

To close the linoleic acid conversion mass balance, residual FAs were quantified using high-performance liquid chromatography (HPLC) [25]. Bromophenacyl bromide (Fluka, Buchs SG, Switzerland) was used to obtain the corresponding esters of FAs after derivatization. A chromatographic method with a UV visible diode array detector (Agilent Technologies, CA, USA) was used to perform the analysis. A C8 column (150 × 2.1 mm ZORBAX Eclipse XDB, 5 μm) was used for the same purpose. The detection wavelength for the esters of FAs was 258 nm. The mobile phase was formed of a mixture of water (A) and acetonitrile + 1% tetrahydrofuran (B) and a solvent gradient of 30% B at 0 min; 70% B at 15 min; and 98% B at 25 min was used.

2.5. Determination of the esterification reaction kinetics

To assess the reaction kinetics, time effect on linoleic acid conversion was measured. A general equation of reaction rate based on the stochiometric products and reactants relationship could be presented as follows (eq. (2)):

$$-r_a = -\frac{1}{S}\frac{dC_{LA}}{dt} = k'.C_{LA}.C_{Me} \quad (2)$$

where r_a is the reaction rate (mg.L^{-1}.m^{-2}.h^{-1}), C_{LA} is the linoleic acid concentration (mg.L^{-1}), C_{Me} that of methanol (mg.L^{-1}), S is the surface area of the solid catalyst (m^2), and k' the reaction rate constant (mg^{-1}.L.m^{-2}.h^{-1}).

Eq. (2) follows a second order reaction rate law. Nevertheless, methanol concentration throughout the reaction could be considered constant due to the excess methanol added to attend the reaction in the direction of the products. Consequently, methanol concentration does not modify the order of the reaction which will behave as a first order reaction and obey pseudo-first order kinetics (eq. (3)) [26,27]:

$$-r_a = -\frac{1}{S}\frac{dC_{LA}}{dt} = k'.C_{LA}.C_{Me} = k.C_{LA} \quad (3)$$

where k (m^{-2}.h^{-1}) = $k'.C_{Me} \approx constant$, when methanol is used in excess.

The initial concentration of linoleic acid is set as $C_{0\ LA}$ at time $t = 0$ and as $C_{t\ LA}$ at time t. The integration of eq. (3) from $t = 0$ to $t = t$, and $C_{0\ LA}$ to $C_{t\ LA}$ gives eq. (4):

$$ln\ C_{0\ LA} - \ln C_{t\ LA} = k.t \quad (4)$$

From the mass balance of the reaction,

$$X_{ML} = 1 - \frac{C_{\ LA}}{C_{0\ LA}}$$

where X_{ML} is the methyl linoleate yield. Upon rearrangement of eqs. (6)–(4), the kinetics of linoleic acid conversion could be expressed as follows (eq. (5)):

$$\ln(1 - X_{ML}) = -k.t \quad (5)$$

3. Results and discussion

3.1. Catalyst characterization

As illustrated in Fig. 1, only signals of crystalline MFI-phase zeolites were observed which confirms the high purity of the 3 zeolite samples.

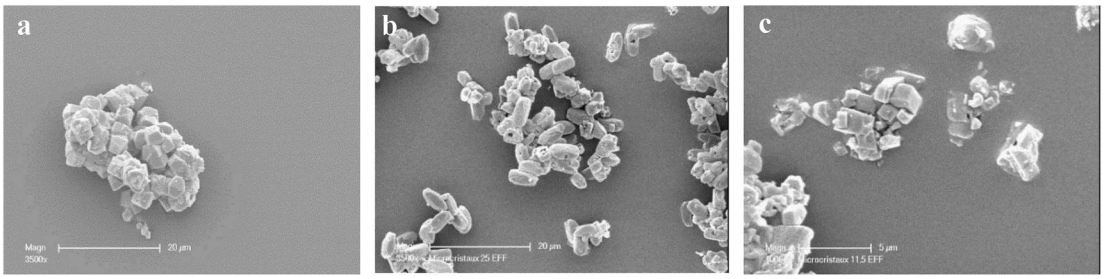

Fig. 2. Scanning electronic microscopy (SEM) images of (a) HZSM-5 (53), (b) HZSM-5 (33.3), and (c) HZSM-5 (14.4).

Table 1
Physico-chemical properties of the H-ZSM5 catalysts.

Zeolites	Si/Al of the sample[a]	Si/Al of the framework[b]	S_{BET} (m^2/g)	Total porous volume (cm^3/g)	Microporous volume (cm^3/g)	[$PyrH^+$][a] (μmol. g^{-1})	[PyrL][b] (μmol. g^{-1})
HZSM-5 (53)	45	53	395	0.17	0.17	351	44
HZSM-5 (33.3)	25	33.3	373	0.15	0.15	347	126
HZSM-5 (14.4)	11.5	14.4	387	0.15	0.15	749	173

[a]Si/Al molar ratio of the sample determined by XRF.
[b]Si/Al molar ratio of the zeolite framework determined from XRF and[27]Al MAS NMR.
[c]Concentration of pyridine adsorbed on Brønsted acid sites following the thermo-desorption at 150 °C.
[d]Concentration of pyridine adsorbed on Lewis acid sites following the thermo-desorption at 150 °C.

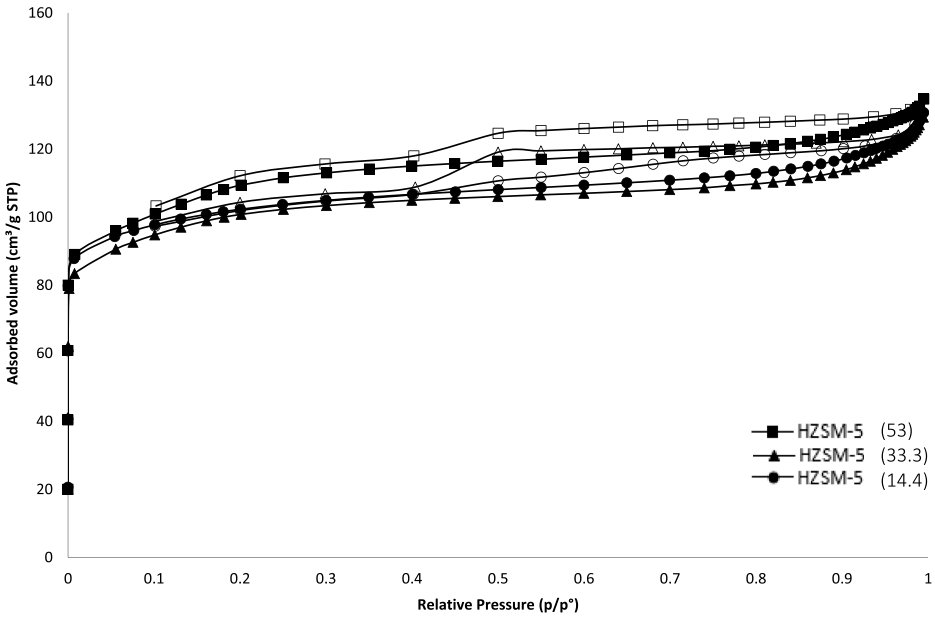

Fig. 3. N_2 adsorption/desorption isotherms at −196 °C of HZSM-5 (53), HZSM-5 (33.3), and HZSM-5 (14.4) samples. Adsorption isotherms (full bullets) and desorption isotherms (empty bullets).

XRD reflections of HZSM-5 (33.3) are broader than those of HZSM-5 (53) and HZSM-5 (14.4). This is explained by the smaller crystal domain that HZSM-5 (33.3) holds as compared to HZSM-5 (53) and HZSM-5 (14.4) as confirmed by SEM imaging.

The SEM micrographs revealed in Fig. 2 show agglomerated prismatic HZSM-5 zeolites particles for the 3 samples. HZSM- 5 (53) crystals have crystal sizes ranging between 3.4 and 7 μm (Fig. 2a). HZSM-5 (33.3) crystals show lower particle sizes of 1.5–5.5 μm (Fig. 2b) while HZSM-5 (14.4) zeolites showed crystal sizes of 2–6 μm (Fig. 2c).

The textural data of the synthesized samples are reported in Table 1. Adsorption-desorption isotherms of type I are obtained for conventional MFI-type zeolites (Fig. 3), which is characteristic for entirely microporous materials. A slight hysteresis was observed for the three zeolite samples, due to the agglomeration of microcrystals and the formation of inter-particular voids in which nitrogen was adsorbed. BET surface areas of the three samples were also similar around 380 $m^2 g^{-1}$. The microporous volume of HZSM-5 (53) sample was 0.17 $cm^3 g^{-1}$ which is very close to the value expected (0.18 $cm^3 g^{-1}$) for a well crystallized MFI microcrystals [30], while a lower value of 0.15 $cm^3 g^{-1}$ was measured for HZSM-5 (33.3) and HZSM-5 (14.4) which correspond to 83.3% of crystallization rate.

[27]Al solid state MAS NMR spectra for the 3 samples were recorded. These samples contained a principal resonance at ca. 56 ppm corresponding to Al species in tetrahedral coordination present in the zeolite

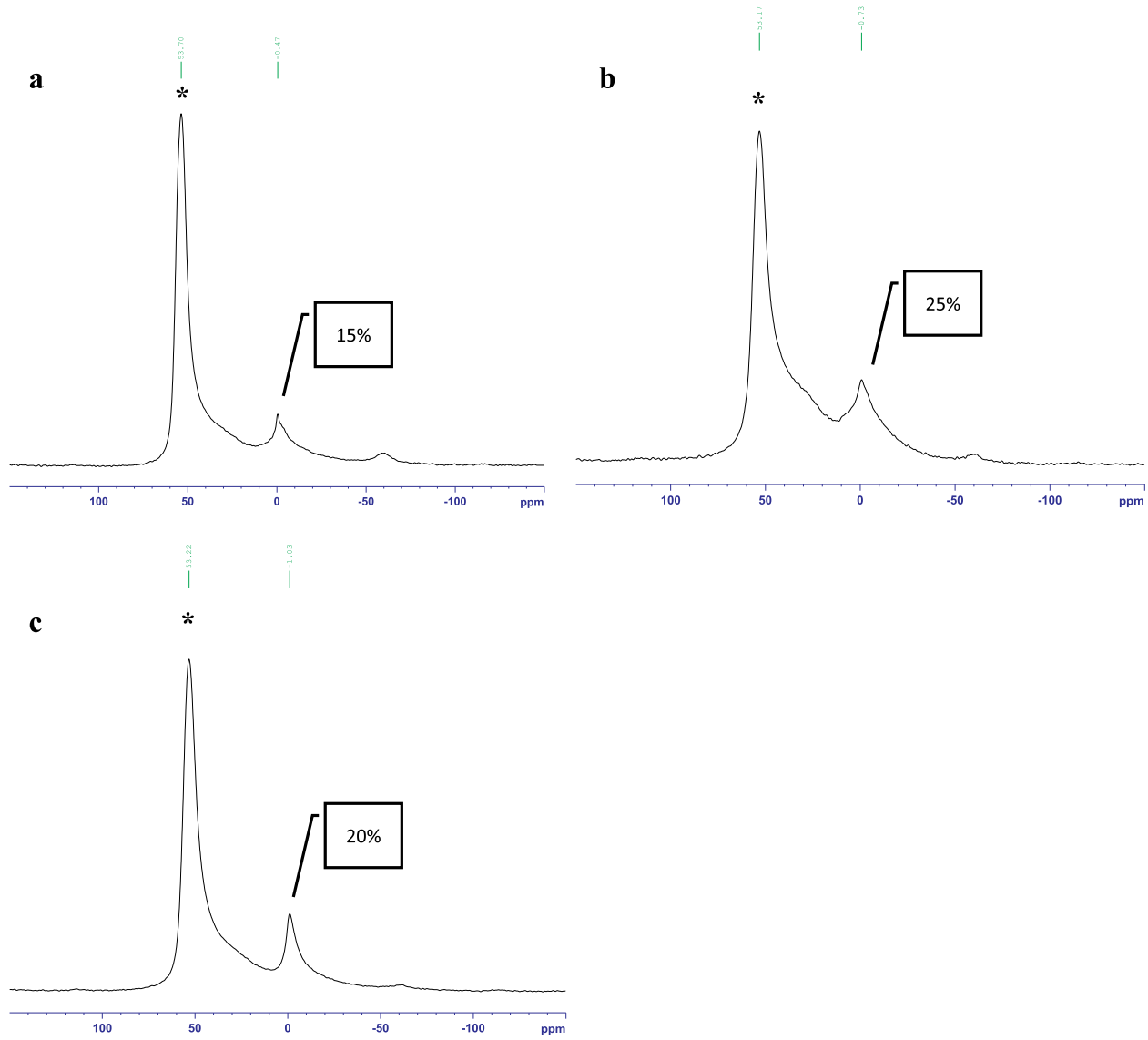

Fig. 4. ^{27}Al MAS NMR spectra of (a) HZSM-5 (53), (b) HZSM-5 (33.3), and (c) HZSM-5 (14.4). (* peak attributed to resonance band).

framework (Fig. 4). ^{27}Al MAS NMR spectra also showed a second resonance around 0 ppm attributed to extra framework Al. HZSM-5 (53), HZSM-5 (33.3), and HZSM-5 (14.4), contain 15%, 25%, and 20% of Al extra framework, respectively (Fig. 4) which coupled to the XRF Si/Al ratios, helped determine the framework Si/Al ratios of the different zeolites (Table 1).

The quantification of the acidity of different Si/Al ratios-HZSM-5 was done by FTIR of adsorbed strong base pyridine molecule. In addition to its ability to access the inner pores of the zeolites, it distinguishes between protonic Brønsted acid sites ($PyrH^+$) and coordinated Lewis acidic sites (PyrL) as it forms pyridium ion on strong Brønsted sites ($PyrH^+$) which mostly contribute to the catalysis of the esterification reaction, and coordinates on weak Lewis acid sites (PyrL) [31]. Bands at 1454 cm^{-1} and 1545 cm^{-1} (Fig. 5) were determined to calculate the concentrations of Lewis and Brønsted acidic sites, respectively and the results are presented in Table 1. Pyridine interacting with both Lewis and Brønsted sites is observed at 1490 cm^{-1} but it does not permit differentiating between the two acidic sites and was thus not used to characterize acidity.

It is interesting to discuss Si/Al ratio effect on zeolite acidity. As Si/Al ratio increases for the HZSM-5 zeolites, acid sites total concentration ($PyrH^+$ and PyrL) decreases, making total acid sites concentration a function of the Si/Al ratio. This is not surprising since as Al content decreases in the zeolite, charge imbalance associated to the Al content also decreases, yielding a lower H^+ exchange capacity. However, the strong Brønsted acidic sites concentrations don't undertake the same trend towards Si/Al ratio for the different zeolites as the total acid sites concentration does.

The concentration of Lewis acid sites in HZSM-5 (53), HZSM-5 (33.3) and HZSM-5 (14.4) correlate fairly well with the extra-framework Al species content of the three samples (Section S1 in supplementary information). Lewis acidity also exists in the intrinsic zeolite framework of HZSM-5 (33.3) and HZSM-5 (14.4).

3.2. Optimized reaction conditions of esterification

3.2.1. Effect of reaction temperature on esterification

Reaction temperature effect on linoleic acid conversion was assessed by conducting experiments with HZSM-5 (53), HZSM-5 (33.3) and HZSM-5 (14.4) using three different temperatures of 60, 140 and 180 °C, under the same reaction conditions (methanol to linoleic acid molar ration = 12/1, stirring rate = 550 rpm, catalyst loading = 10 wt%, and reaction time = 6 h). As shown in Fig. 6, catalytic activity increased with increasing temperature except for HZSM-5 (53) and HZSM-5 (33.3)

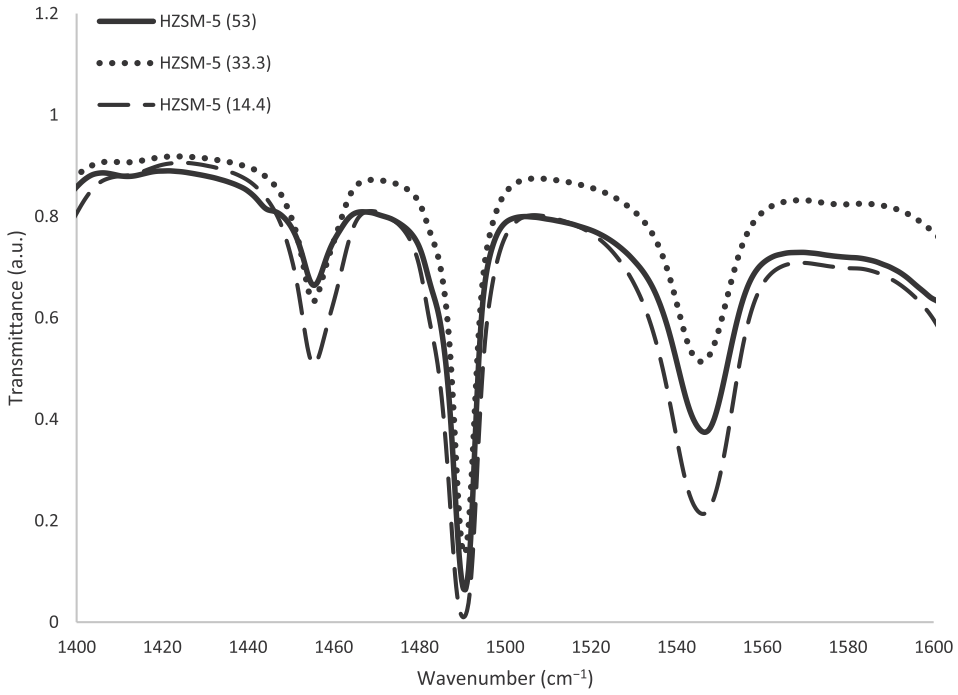

Fig. 5. FTIR spectra after zeolites saturation with pyridine and desorption at 150 °C.

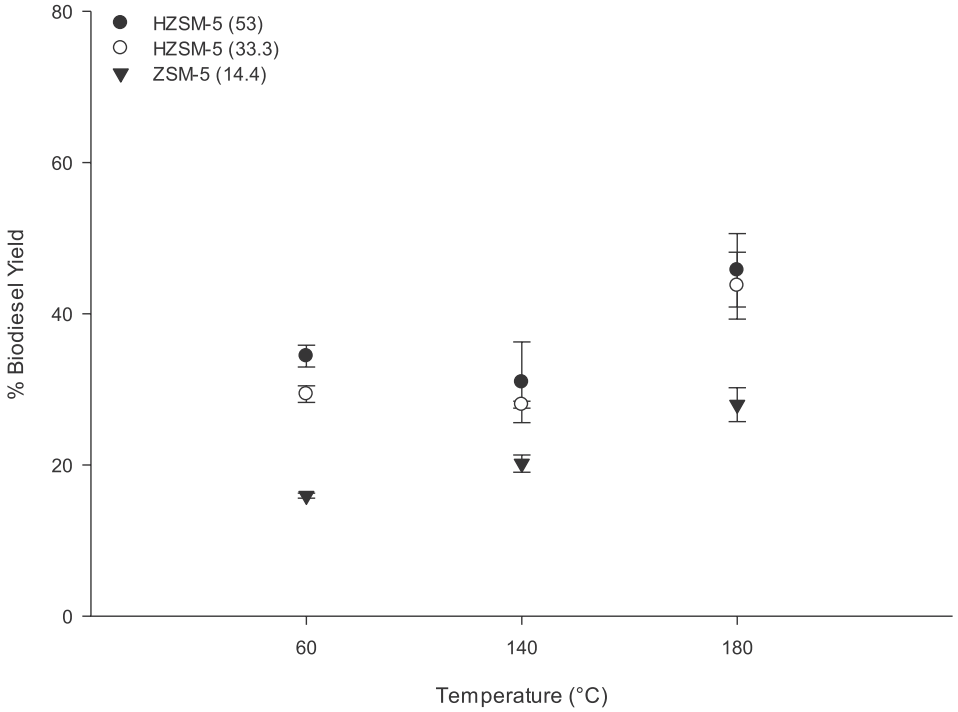

Fig. 6. Reaction temperature variation effect on the esterification of linoleic acid using HZSM-5 (53), HZSM-5 (33.3), and HZSM-5 (14.4) catalysts at the molar ratio of methanol to linoleic acid molar ratio of 12:1, catalyst loading of 10 wt%, stirring rate of 550 rpm, and reaction time of 6 h.

which showed no significant difference in linoleic conversion when the reaction temperature changed from 60 to 140 °C. Measured FAMEs yield for HZSM-5 (53) and HZSM-5 (33.3), was, respectively, 34.40% (standard deviation (SD) = 1.18) and 29.36% (SD = 0.89) at 60 °C, and 31.83% (SD = 4.36) and 27.96% (SD = 0.38) at 140 °C. For all zeolites, the highest linoleic acid conversions were reached at the optimal reaction temperature of 180 °C, with the order of conversion being HZSM-5 (53) (45.76%, SD = 4.85) ˃ HZSM-5 (33.3) (43.73%, SD = 4.43) ˃ HZSM-5 (14.4) (27.96%, SD = 2.23). Higher temperatures achieved higher conversions which is explained by the decrease of the FA viscosity at high temperatures, promoting thus a better methanol/linoleic acid phase mixture, increasing thus methyl linoleate yield. It is noteworthy to mention that at the different reaction temperatures used, linoleic acid conversions using HZSM-5 (53) were the highest, followed by HZSM-5 (33.3) and HZSM-5 (14.4), respectively. While HZSM-5 (14.4) has the highest strong Brønsted acid sites concentration, it exhibits the lower

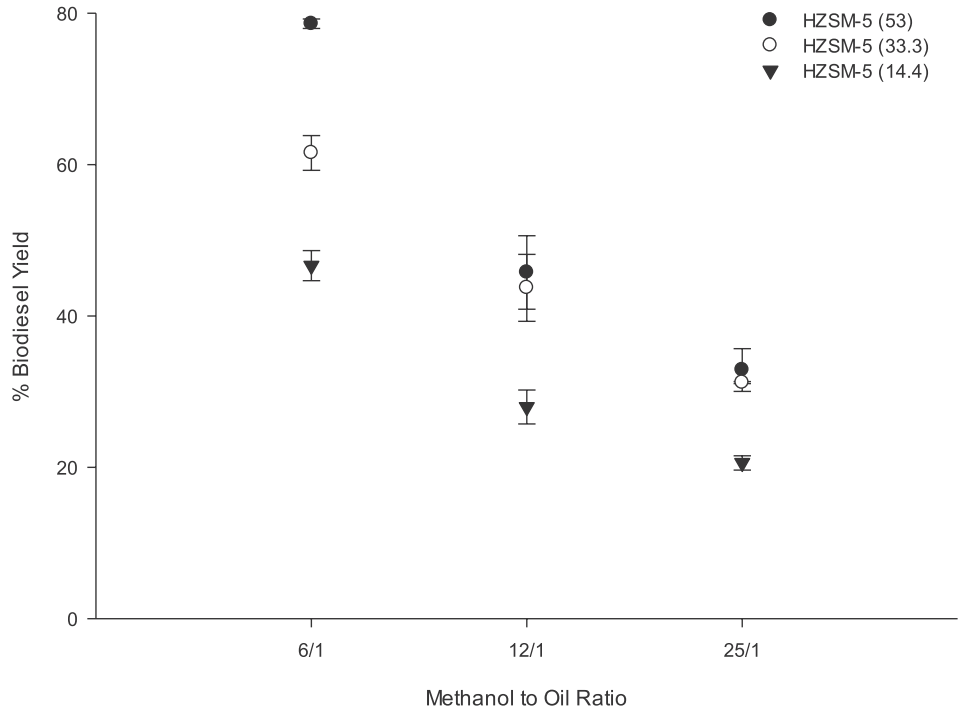

Fig. 7. Methanol to linoleic acid molar ratio variation effect on the esterification of linoleic acid using HZSM-5 (53), HZSM-5 (33.3), and HZSM-5 (14.4) catalysts at catalyst loading of 10 wt%, reaction temperature of 180 °C, stirring rate of 550 rpm and reaction time of 6 h.

catalytic performance. The increase of Brønsted acidity doesn't seem to be the only factor affecting the conversions obtained, as will be later discussed.

3.2.2. Effect of methanol to linoleic acid ratio on esterification

For the different types of tested catalysts, the effect of methanol to linoleic acid molar ratio on the conversion of linoleic acid was evaluated by varying the volume of methanol used. Methanol to linoleic acid molar ratios of 6:1, 12:1, and 25:1 were used to provide excess methanol to direct the reversible esterification reaction towards the production of methyl linoleate [32]. Similar reaction conditions were used for the esterification reactions and consisted of 10 wt% catalyst loading, 6 h reaction time, 550 rpm stirring rate, and fixed optimal temperature of 180 °C. Fig. 7 shows that linoleic acid conversion rate decreased for all zeolite catalysts as the molar ratio of methanol to linoleic acid increased from 6:1 to 12:1 and from 12:1 to 25:1. While it is expected that at increased methanol to linoleic acid molar ratios the equilibrium shifts towards the direction of methyl esters formation [33], the influence of reverse reaction was in this case potentially greater than the forward esterification reaction. This phenomenon is due to the slight recombination of methyl linoleate and water to form linoleic acid. Excess methanol could increase the miscibility of water in methyl linoleate favoring thus the backward reaction to take place [31]. Also, the conversion may have decreased due to the adsorption of more water produced when the quantity of methanol was further increased to react with linoleic acid. The optimal molar ratio of methanol to linoleic acid was 6:1 with an order of conversion of HZSM-5 (53) (78.62%, SD = 0.63) > HZSM-5 (33.3) (61.56%, SD = 2.30) > HZSM-5 (14.4) (27.96%, SD = 1.99).

For all the experiments carried out, residual linoleic acid was quantified using HPLC and mass balance closure was inspected. Section 2 in supplementary information presents numeric methyl esters yields and residual linoleic acid content at the different reaction conditions.

3.2.3. Effect of external mass transfer limitation

Microporous HZSM-5 zeolites have a small pore size (5.1–5.5 Å) and linoleic acid molecules possess a kinetic diameter of 8.08 Å estimated using eq. (6) [32].

$$\sigma = 1.234.(M_W)^{1/3} \quad (6)$$

where σ is the kinetic diameter estimated for hydrocarbon molecules, and M_W is the molecular weight of linoleic acid in g mol^{-1}.

Meaning that it is unlikely for such a molecule to penetrate the pores and reach the internal active sites of the microporous zeolite such as microporous HZSM-5.

Therefore, the esterification reaction is more likely to happen on the external surface of microporous HZSM-5 [36,37]. However, the mass transfer amid the bulk fluid and the external catalytic surface should be examined. In a homogeneous catalytic reaction, the effect of mass transfer is negligible, as all substances (reactants, catalysts and products) are in one phase. However, the catalyst does not belong to the same phase of the reactants in a catalytic heterogeneous reaction as is the case in this study, and reactants diffusion from the bulk phase to the external catalyst particle surface could be hindered if proper stirring is not provided.

At 550 rpm rate of stirring, the external mass transfer limitation effect is determined by the dimensionless Mears criterion (C_M) [38]:

$$C_M = \frac{r_0\, \rho\, d\, n}{2\, k_c\, C_0} \quad (7)$$

where, r_0 is the initial reaction rate that is equal to the linoleic acid esterification rate at 60 min $\left(= \frac{moles\ of methyl\ esters\ produced\ in\ the\ reaction\ time(mol)}{catalyst\ loading(g)\ \times reaction\ time(min)}\right)$ [36], ρ is the density of the HZSM-5 matrix, d is the mean diameter of the catalyst, n is the reaction order (the esterification reaction obeyed the pseudo first-order reaction kinetics as shown in Section S3 (supplementary information) reaction coefficients of $3.63 \times 10^{-1}\, m^{-2}\, h^{-1}$, $2.20 \times 10^{-1}\, m^{-2}\, h^{-1}$, and $1.79 \times 10^{-1}\, m^{-2}\, h^{-1}$ for HZSM-5 (53), HZSM-5 (33.3) and HZSM-5 (14.4), respectively), C_0 is the linoleic acid initial concentration, and k_c is the mass transfer coefficient, calculated using the equation developed by Dwivedi and Upadhyay [40]:

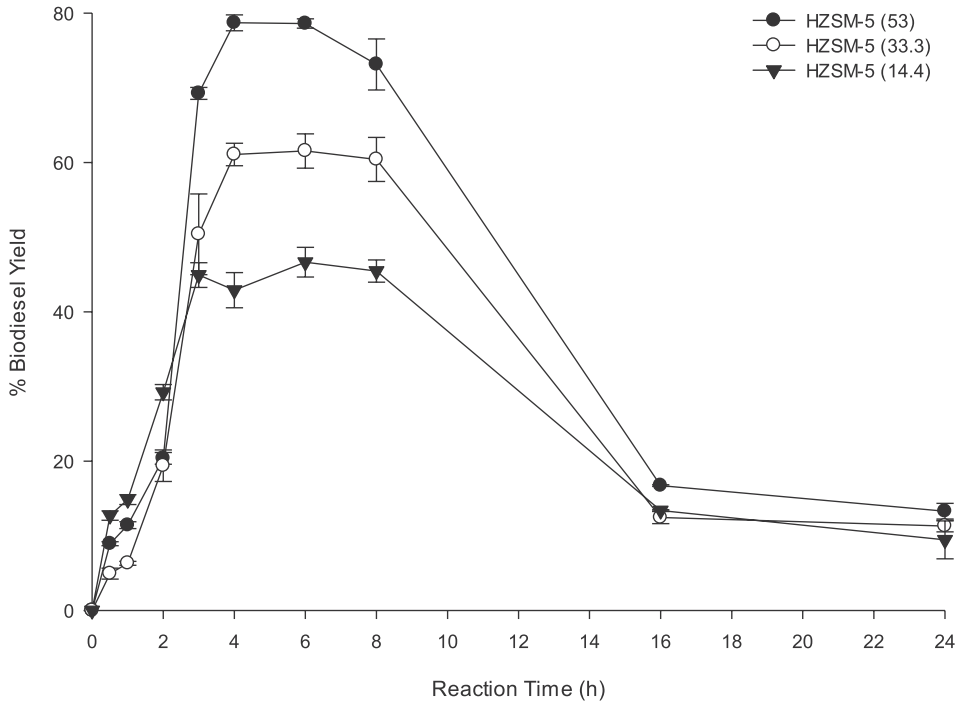

Fig. 8. Reaction time effect on the esterification of linoleic acid using HZSM-5 (53), HZSM-5 (33.3), and HZSM-5 (14.4) catalysts at catalyst loading of 10 wt%, methanol to linoleic molar ratio of 6:1, reaction temperature of 180 °C, and stirring rate of 550 rpm.

$$k_c = \frac{2D_{AB}}{d_z} + 0.31 N_S^{\frac{2}{3}} \left(\frac{\Delta\rho\, \mu_c\, g}{\rho_c^2} \right)^{1/3} \quad (8)$$

where D_{AB} is the molecular diffusion coefficient of solute A (linoleic acid) at low concentration in solvent B (methanol), calculated based on the Wilke-Chang method, accounting for the reaction temperature of 180 °C [41], μ_c is the solvent viscosity, d_z is the catalyst particle diameter, N_S is the Schmidt number, g is the gravitational acceleration, and $\Delta\rho$ is the variation between the catalyst and the solution densities and ρ_c is the solvent density.

In the kinetic study, the external mass transfer diffusion resistance is insignificant when the Mears criterion value is lower than 0.15. C_M were 2.71×10^{-7}, 1.35×10^{-7}, and 2.84×10^{-7} for HZSM-5 (53), HZSM-5 (33.3) and HZSM-5 (14.4) respectively. This indicates that the solid-liquid interface-external mass transfer limitations were surmounted when the stirring speed was 550 rpm and that the esterification reaction mostly happened on the totality of the external surface of the zeolite.

3.2.4. Effect of reaction time on esterification

Reaction time effect on the conversion of linoleic acid was studied by carrying out experiments using HZSM-5 (53), HZSM-5 (33.3), HZSM-5 (14.4) catalysts at the optimal reaction conditions (catalyst loading of 10%, reaction temperature of 180 °C, methanol to linoleic acid molar ratio of 6:1, and stirring rate of 550 rpm) with a reaction time variation in the range of 0–24 h. Fig. 8 displays the reaction time effect on methyl linoleate yield for the different Si/Al ratio catalysts. According to the results, an increase in the reaction time from 0.5 to 4 h shows a noticeable linoleic acid conversion increase which reached respective maxima of 79.78% and 62.60% for HZSM-5 (53) and HZSM-5 (33.3) at 4 h. For these two zeolites, no further significantly different conversion was observed from 4 to 8 h, making thus the 4 h the optimal reaction time for the model reaction of biodiesel. A maximum yield of 48.66% was however achieved at 6 h reaction time for HZSM-5 (14.4). The general increase in catalytic performance for the HZSM-5 zeolites of higher Si/Al ratios will be explained in detail below. A decrease in the methyl ester yield was significant after 16 h of the reaction. Extended heating times of linoleic acid had resulted in its polymerization. A rubber-like deposit which remained insoluble in DCM was found at the bottom of the reactor. Aside from yielding lower linoleic acid conversions, higher reaction times are not favorable for the esterification reactions due to the higher energy consumption they require.

3.2.5. Effect of Si/Al ratio on esterification

The difference in performance between HZSM-5 zeolites with different Si/Al ratios is interesting (Fig. 8). At early stages of the esterification reactions (up to 2 h), a higher catalytic activity was detected for the HZSM-5 zeolite with the lower Si/Al, agreeing with the fact that the activity improves as the Brønsted acid sites amount increases (at lower Si/Al ratios). After 4 h, linoleic acid activity on zeolites increased with increasing Si/Al ratio. Doyle et al. found a similar increase in activity for the HY zeolites with lower Si/Al ratio, during the initial stages of the reaction [18]. However, a lower Si/Al ratio gives the zeolite a more hydrophilic character allowing surface adsorption of water produced from the esterification reactions and blocking thus the access of the fatty acids to the external active sites. As water is produced, it competes with less polar methanol and linoleic acid for the adsorption sites of the zeolites surface. This explains the lower linoleic acid conversions registered for the more hydrophilic HZSM-5 (14.4) zeolites after 4 h reaction time. Ben Mya et al. [42] concluded that hydrophilic zeolites absorb high quantities of water which inhibit the conversion of FAs in esterification reactions. On another hand, although zeolite acidity decreases with increasing Si/Al ratio, their hydrophobicity increases, allowing them to rapidly desorb the produced water during the esterification reaction which could lead to the catalyst deactivation. This results in an increase in the surface coverage of linoleic acid. Liu et al. [43] reviewed solid acids development with suitable hydrophobicity to enhance catalytic activities in reactions such as the esterification reaction. Therefore, Si/Al ratio of HZSM-5 determines the acidity and relative hydrophobic character of the zeolite, both influencing the kinetics and ultimate yield from the esterification reactions. Similarly, Prinsen et al. [44] showed that the conversion of palmitic acid was dependent on the hydrophobic/hydrophilic character of the microporous zeolite and reactants.

At initial phases of the esterification reaction the acidity of the zeolites took over the hydrophilic character of HZSM-5 (14.4) as water

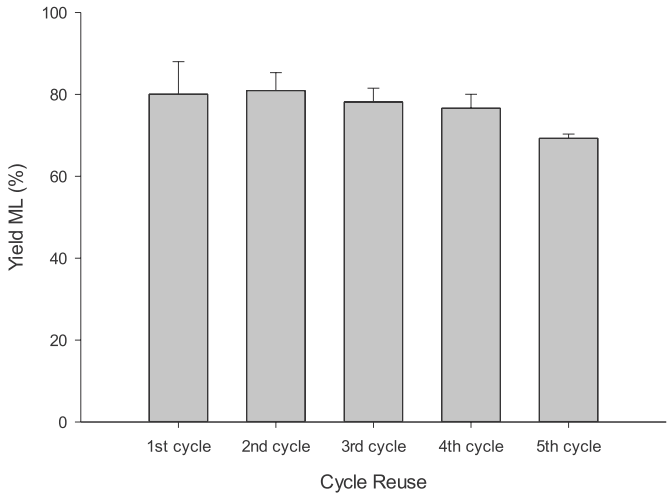

Fig. 9. Methyl ester yield after HZSM-5 (53) reuse in linoleic acid esterification.

molecules were not yet produced in quantities high enough to compete with linoleic acid adsorption to acid sites. HZSM-5 (14.4) registered a maximum conversion of 30.28% at 2 h reaction time in comparison with 21.49% and 21.15% for HZSM-5 (33.3) and HZSM-5 (53), respectively. However, at later stages of the reactions (beyond 4 h), the relative hydrophobic character of HZSM-5 zeolites allowed rapid desorption of produced water molecules and more coverage of linoleic acid which resulted in higher methyl esters production) yields despite the lower acidity. Linoleic acid conversion reached a maximum of 79.78% and 62.60% for HZSM-5 (53) and HZSM-5 (33.3) at 4 h reaction time, respectively, whereas it only reached a maximum of 45.27% at a similar reaction time for HZSM-5 (14.4). Thus, HZSM-5 (14.4) zeolite exhibited the highest acidity but the lower catalytic adaptability, and the zeolites with high Si/Al ratios showed better catalytic efficiency.

3.2.6. Catalyst regeneration

The ability of HZSM-5 (53) catalyst reusability was assessed by performing five successive 4 h linoleic acid esterification cycles at methanol, linoleic acid molarities and reaction temperature similar to the optimum conditions obtained in this study. Subsequent to each cycle, gravitational filtration was performed to separate the used catalyst from the liquid reaction. The catalyst was then heated in air at 105 °C for 6 h. The liquid product mixture yielded around 80% for the first 4 cycles and decreased to 68.25 (SD = 0.84) at the end of the 5th cycle (Fig. 9). This shows that HZSM-5 (53) catalyst retains catalytic activity after 5 consecutive cycles despite the slight methyl esters decrease.

4. Conclusion

Esterification of linoleic acid with methanol was performed over HZSM-5 zeolites with distinct Si/Al ratios. A maximum methyl ester yield of 79.78% was reached for the esterification of linoleic acid using HZSM-5 (53) at 4 h reaction time, 10 wt% catalyst loading, 6:1 methanol to linoleic acid molar ratio and 180 °C and maintained after 4 consecutive reaction cycles after catalyst regeneration, with a slight decrease to 68.25% at the end of the fifth cycle. decreasing Si/Al ratio of HZSM-5 zeolites increases their acidity and decreases their hydrophobic character with a consequent effect on the esterification reactions. As the reaction time progresses, water molecules are produced and are rapidly adsorbed to more hydrophilic surfaces (zeolites with low Si/Al), decreasing the surface coverage of linoleic acid and yielding lower conversions despite the zeolites higher acidity. Linoleic acid conversion rate with methanol can thus be improved by synthesizing zeolites with adequate relative hydrophobicity and acidity.

Declaration of competing interest

The authors declare that they have no known competing financial interests or personal relationships that could have appeared to influence the work reported in this paper.

Acknowledgment

This research was supported by the University Research Board (URB) at the American University of Beirut, Lebanon.

Appendix A. Supplementary data

Supplementary data to this article can be found online at https://doi.org/10.1016/j.micromeso.2019.109855.

References

[1] G. Baskar, R. Aiswarya, Trends in catalytic production of biodiesel from various feedstocks, Renew. Sustain. Energy Rev. 57 (2016) 496–504, https://doi.org/10.1016/j.rser.2015.12.101.
[2] S.B. Živković, M.V. Veljković, I.B. Banković-Ilić, I.M. Krstić, S.S. Konstantinović, S. B. Ilić, J.M. Avramović, O.S. Stamenković, V.B. Veljković, Technological, technical, economic, environmental, social, human health risk, toxicological and policy considerations of biodiesel production and use, Renew. Sustain. Energy Rev. 79 (2017) 222–247, https://doi.org/10.1016/j.rser.2017.05.048.
[3] Z. Yaakob, B.N. Narayanan, S. Padikkaparambil, K.S. Unni, P.M. Akbar, A review on the oxidation stability of biodiesel, Renew. Sustain. Energy Rev. 35 (2014) 136–153, https://doi.org/10.1016/j.rser.2014.03.055.
[4] M.L. Granados, M.D.Z. Poves, D.M. Alonso, R. Mariscal, F.C. Galisteo, R. Moreno-Tost, J. Santamaría, J.L.G. Fierro, Biodiesel from sunflower oil by using activated calcium oxide, Appl. Catal. B Environ. 73 (2007) 317–326, https://doi.org/10.1016/j.apcatb.2006.12.017.
[5] Y.H. Tan, M.O. Abdullah, C. Nolasco-Hipolito, The potential of waste cooking oil-based biodiesel using heterogeneous catalyst derived from various calcined eggshells coupled with an emulsification technique: a review on the emission reduction and engine performance, Renew. Sustain. Energy Rev. 47 (2015) 589–603, https://doi.org/10.1016/j.rser.2015.03.048.
[6] V.B. Veljković, I.B. Banković-Ilić, O.S. Stamenković, Purification of crude biodiesel obtained by heterogeneously-catalyzed transesterification, Renew. Sustain. Energy Rev. 49 (2015) 500–516, https://doi.org/10.1016/j.rser.2015.04.097.
[7] K.H. Chung, D.R. Chang, B.G. Park, Removal of free fatty acid in waste frying oil by esterification with methanol on zeolite catalysts, Bioresour. Technol. 99 (2008) 7438–7443, https://doi.org/10.1016/j.biortech.2008.02.031.
[8] K. Saravanan, B. Tyagi, R.S. Shukla, H.C. Bajaj, Esterification of palmitic acid with methanol over template-assisted mesoporous sulfated zirconia solid acid catalyst, Appl. Catal. B Environ. 172–173 (2015) 108–115, https://doi.org/10.1016/j.apcatb.2015.02.014.
[9] Y.-M. Park, S.-H. Chung, H.J. Eom, J.-S. Lee, K.-Y. Lee, Tungsten oxide zirconia as solid superacid catalyst for esterification of waste acid oil (dark oil), Bioresour. Technol. 101 (2010) 6589–6593, https://doi.org/10.1016/j.biortech.2010.03.109.
[10] Y. Feng, B. He, Y. Cao, J. Li, M. Liu, F. Yan, X. Liang, Biodiesel production using cation-exchange resin as heterogeneous catalyst, Bioresour. Technol. 101 (2010) 1518–1521, https://doi.org/10.1016/j.biortech.2009.07.084.
[11] J. Gardy, A. Hassanpour, X. Lai, M.H. Ahmed, M. Rehan, Biodiesel production from used cooking oil using a novel surface functionalised TiO 2 nano-catalyst, Appl. Catal. B Environ. 207 (2017) 297–310, https://doi.org/10.1016/j.apcatb.2017.01.080.
[12] L. Shirazi, E. Jamshidi, M.R. Ghasemi, The effect of Si/Al ratio of ZSM-5 zeolite on its morphology, acidity and crystal size, Cryst. Res. Technol. 43 (2008) 1300–1306, https://doi.org/10.1002/crat.200800149.
[13] S. Sang, F. Chang, Z. Liu, C. He, Y. He, L. Xu, Difference of ZSM-5 zeolites synthesized with various templates, Catal. Today 93–95 (2004) 729–734, https://doi.org/10.1016/j.cattod.2004.06.091.
[14] C. Falamaki, M. Edrissi, M. Sohrabi, Studies on the crystallization kinetics of zeolite ZSM-5 with 1,6-hexanediol as a structure-directing agent, Zeolites 19 (1997) 2–5, https://doi.org/10.1016/S0144-2449(97)00025-0.
[15] K.-H. Chung, B.-G. Park, Esterification of oleic acid in soybean oil on zeolite catalysts with different acidity, J. Ind. Eng. Chem. 15 (2009) 388–392, https://doi.org/10.1016/j.jiec.2008.11.012.
[16] W. Meng, X. Wang, Z. Xiao, J. Wang, D.B. Mitzi, Y. Yan, Parity-forbidden transitions and their impact on the optical absorption properties of lead-free metal halide perovskites and double perovskites, J. Phys. Chem. Lett. 8 (2017) 2999–3007, https://doi.org/10.1021/acs.jpclett.7b01042.
[17] K. Sun, J. Lu, L. Ma, Y. Han, Z. Fu, J. Ding, A comparative study on the catalytic performance of different types of zeolites for biodiesel production, Fuel 158 (2015) 848–854, https://doi.org/10.1016/j.fuel.2015.06.048.

[18] A.M. Doyle, T.M. Albayati, A.S. Abbas, Z.T. Alismaeel, Biodiesel production by esterification of oleic acid over zeolite Y prepared from kaolin, Renew. Energy 97 (2016) 19–23, https://doi.org/10.1016/j.renene.2016.05.067.
[19] K.A. Tarach, K. Góra-Marek, J. Martinez-Triguero, I. Melián-Cabrera, Acidity and accessibility studies of desilicated ZSM-5 zeolites in terms of their effectiveness as catalysts in acid-catalyzed cracking processes, Catal. Sci. Technol. 7 (2017) 858–873, https://doi.org/10.1039/C6CY02609E.
[20] J. Dhainaut, T.J. Daou, Y. Bidal, N. Bats, B. Harbuzaru, G. Lapisardi, H. Chaumeil, A. Defoin, L. Rouleau, J. Patarin, One-pot structural conversion of magadiite into MFI zeolite nanosheets using mononitrogen surfactants as structure and shape-directing agents, CrystEngComm 15 (2013) 3009, https://doi.org/10.1039/c3ce40118a.
[21] W.J. Kim, S.D. Kim, U.S. Patents 7 (2008) 361.
[22] K.S. Walton, R.Q. Snurr, Applicability of the BET method for determining surface areas of microporous Metal−Organic frameworks, J. Am. Chem. Soc. 129 (2007) 8552–8556, https://doi.org/10.1021/ja071174k.
[23] S. K, J. Rouquerol, F. Rouquerol, P. Llewellyn, G. Maurin, Sing, Adsorption by Powders and Porous Solids: Principles, Methodology and Applications, 2013.
[24] M.J. Guisnet, P. Ayrault, Datka, Acid properties of dealuminated mordenites studied by IR spectroscopy. 2. Concentration, acid strength and heterogeneity of OH groups, Pol. J. Chem. 71 (1997) 1455–1461.
[25] A. Astafan, Y. Pouilloux, J. Patarin, N. Bats, C. Bouchy, T. Jean Daou, L. Pinard, Impact of extreme downsizing of *BEA-type zeolite crystals on n-hexadecane hydroisomerization, New J. Chem. 40 (2016) 4335–4343, https://doi.org/10.1039/C5NJ02837J.
[26] D. Massiot, F. Fayon, M. Capron, I. King, S. Le Calvé, B. Alonso, J.-O. Durand, B. Bujoli, Z. Gan, G. Hoatson, Modelling one- and two-dimensional solid-state NMR spectra, Magn. Reson. Chem. 40 (2002) 70–76, https://doi.org/10.1002/mrc.984.
[27] A. Gratzfeld-Husgen, R. Schuster, HPLC for Food Analysis. A Primer, Agil. Technol., 2001.
[30] I. Kabalan, B. Lebeau, H. Nouali, J. Toufaily, T. Hamieh, B. Koubaissy, J.-P. Bellat, T.J. Daou, New generation of zeolite materials for environmental applications, J. Phys. Chem. C 120 (2016) 2688–2697, https://doi.org/10.1021/acs.jpcc.5b10052.
[31] E.G. Derouane, J.C. Védrine, R.R. Pinto, P.M. Borges, L. Costa, M.A.N.D.A. Lemos, F. Lemos, F.R. Ribeiro, The acidity of zeolites: concepts, measurements and relation to catalysis: a review on experimental and theoretical methods for the study of zeolite acidity, Catal. Rev. 55 (2013) 454–515, https://doi.org/10.1080/01614940.2013.822266.
[32] F. Qiu, Y. Li, D. Yang, X. Li, P. Sun, Heterogeneous solid base nanocatalyst: preparation, characterization and application in biodiesel production, Bioresour. Technol. 102 (2011) 4150–4156, https://doi.org/10.1016/j.biortech.2010.12.071.
[33] W. Xie, L. Zhao, Heterogeneous CaO–MoO3–SBA-15 catalysts for biodiesel production from soybean oil, Energy Convers. Manag. 79 (2014) 34–42, https://doi.org/10.1016/j.enconman.2013.11.041.
[36] S.S. Vieira, Z.M. Magriotis, M.F. Ribeiro, I. Graça, A. Fernandes, J.M.F.M. Lopes, S. M. Coelho, N.A.V. Santos, A.A. Saczk, Use of HZSM-5 modified with citric acid as acid heterogeneous catalyst for biodiesel production via esterification of oleic acid, Microporous Mesoporous Mater. 201 (2015) 160–168, https://doi.org/10.1016/j.micromeso.2014.09.015.
[37] S.S. Vieira, Z.M. Magriotis, I. Graça, A. Fernandes, M.F. Ribeiro, J.M.F.M. Lopes, S. M. Coelho, N.A.V. Santos, A.A. Saczk, Production of biodiesel using HZSM-5 zeolites modified with citric acid and SO42−/La2O3, Catal. Today 279 (2017) 267–273, https://doi.org/10.1016/j.cattod.2016.04.014.
[38] I.B. Ju, H.-W. Lim, W. Jeon, D.J. Suh, M.-J. Park, Y.-W. Suh, Kinetic study of catalytic esterification of butyric acid and n-butanol over Dowex 50Wx8-400, Chem. Eng. J. 168 (2011) 293–302, https://doi.org/10.1016/j.cej.2010.12.086.
[40] P.N. Dwivedi, S.N. Upadhyay, Ind. Eng. Chem. Process Des. Dev. 16 (1977) 157–165.
[41] C.R. Wilke, P. Chang, AIChE J. 1 (1955) 264–270.
[42] O. Ben Mya, M. Bita, I. Louafi, A. Djouadi, Esterification process catalyzed by ZSM-5 zeolite synthesized via modified hydrothermal method, Methods 5 (2018) 277–282, https://doi.org/10.1016/j.mex.2018.03.004.
[43] F. Liu, K. Huang, A. Zheng, F.-S. Xiao, S. Dai, Hydrophobic solid acids and their catalytic applications in green and sustainable chemistry, ACS Catal. 8 (2018) 372–391, https://doi.org/10.1021/acscatal.7b03369.
[44] P. Prinsen, R. Luque, C. González-Arellano, Zeolite catalyzed palmitic acid esterification, Microporous Mesoporous Mater. 262 (2018) 133–139, https://doi.org/10.1016/j.micromeso.2017.11.029.